RSC Advances

PAPER

View Article Online
View Journal | View Issue

Cite this: *RSC Adv.*, 2020, **10**, 30169

Parameter control and property analysis in the preparation of platinum iodide nanocolloids through the electrical spark discharge method

Kuo-Hsiung Tseng, *[a] Zih-Yuan Lin,[a] Meng-Yun Chung,[a] Der-Chi Tien[a] and Leszek Stobinski[b]

Received 5th May 2020
Accepted 10th August 2020

DOI: 10.1039/d0ra04048g

rsc.li/rsc-advances

This study employed the electrical spark discharge method to prepare platinum iodide nanocolloids at normal temperature and pressure. Wires composed of 99.5% platinum were applied as the electrodes, and 250 ppm liquid iodine was employed as the dielectric fluid. An electric discharge machine was applied to generate cyclic direct current pulse power between the electrodes. Five sets of turn-on and turn-off time (T_{on}–T_{off}) parameters, namely 10–10, 30–30, 50–50, 70–70, and 90–90 μs, were implemented to identify the optimal nanocolloid preparation conditions. An ultraviolet-visible spectroscope, a Zetasizer, and a transmission electron microscope were used to examine the nanocolloids' properties. The results revealed that the T_{on}–T_{off} parameter set of 10–10 μs was the most ideal setting for platinum iodide nanocolloid preparation. With this parameter set, the characteristic wavelengths of the nanocolloid were 285 and 350 nm, respectively; its absorbance values were 0.481 and 0.425, respectively; and its zeta potential and particle size were −30.3 mV and 61.88 nm, respectively. This parameter set yielded maximized absorbance, satisfactory suspension stability, and minimized nanoparticle sizes for the nanocolloid.

1 Introduction

Platinum exhibits extremely stable chemical properties, high density, excellent ductility, and a high melting point. It is highly resistant to oxidants, acids, and alkalis. Platinum is rare on Earth and is therefore expensive. Platinum has a broad range of applications. Generally, platinum is used as a precious metal in jewelry processing. It is used as a material for electrodes in industrial applications,[1,2] it is applied as a catalyst in chemical industries,[3,4] and it is incorporated into the manufacturing of advanced thin film sensors that accurately measure surface temperature and heat flux in the aerospace industry.[5] In physics, platinum is employed to produce organic light-emitting diodes.[6] Platinum is broadly applied in medicine,[7,8] including various cancer and drug treatments,[9–11] with spectacular results. Iodine is a nonmetallic chemical element and a nonartificial stable halogen. In medicine, iodine is prevalently used for disinfecting wounds, including surgical disinfection. As one of the many available antibacterial agents, iodine has, for decades, been commonly applied as a preservative and for wound healing because of its excellent efficacy and tolerance.[12] In the field of material science, iodine is used to improve the capacity of rechargeable batteries by increasing their energy density; it is also used to enhance the power generation efficiency of solar cells.[13,14]

Platinum is applied in many other fields, most of which involve chemical preparation.[15,16] Chemical preparation can generate by products that damage the environment and human health. By contrast, the Electrical Spark Discharge Method (ESDM) is a green alternative for the preparation of platinum nanoparticles.[17] Its efficiency and cleanliness renders ESDM suitable for the preparation of platinum iodide nanocolloids. ESDM facilitates spark discharge through the energy generated in a strong electric field when two electrodes are approximately 30 μm apart.[18] Through the high-frequency voltage pulse from the two electrodes, electrical energy is converted to thermal energy, which melts workpieces and removes the material from their surfaces, forming nanoparticles. This study employed an electric discharge machine (EDM) to prepare platinum iodide nanocolloids. Platinum wires were applied as electrodes, and 200 mL of 250 ppm liquid iodine was used as the dielectric fluid. A magnetic stirrer was employed to evenly disperse platinum nanoparticles in the dielectric fluid. Preparation parameters were then adjusted to identify the optimal conditions for the preparation of nanocolloids with high concentration and suspension stability. An ultraviolet-visible spectroscope (UV-vis), a Zetasizer, and a transmission electron microscope (TEM) were employed to verify the properties of the platinum iodide nanocolloids.

[a]*Department of Electrical Engineering, National Taipei University of Technology, Taiwan, Republic of China. E-mail: khtseng@ee.ntut.edu.tw*

[b]*Materials Chemistry, Warsaw University of Technology, Warynskiego 1, 00-645 Warsaw, Poland*

2 Material and methods

A Nanocolloid preparation system

Fig. 1(a) illustrates the EDM used for the preparation of platinum iodide nanocolloids. The upper and lower electrodes consisted of 99.5% platinum and the dielectric fluid 200 mL of 250 ppm liquid iodine, prepared through the mixture of 199.5 mL of deionized water and 0.5 mL of 10% w/v iodine. The electrodes were immersed in the fluid, and the distance between them was controlled using a servo control system to create an arc for electric discharge machining. A lamp was used to observe the preparation process, and a magnetic stirrer was applied to evenly disperse the platinum nanoparticles in the fluid.

Fig. 1(b) depicts the EDM control panel. In a general preparation process, the nonload preparation voltage output is 140 V, but it can be switched to 240 V using a "HV" switch for the preparation of metals with high hardness and melting temperatures. The "CAPACITOR" can be adjusted to 0.1, 0.5, or 1 μF. Adding the capacitor to the discharge power source increases the modulation voltage of T_{on}, thereby reinforcing the metal-melting process. This can be applied to metals with low conductivity. The "T_{on}–T_{off}" represents the duty cycle of the discharge between the electrodes, ranging between 0 and 999 μs, and adjusting this affects the discharge success rate and preparation speed. Studies have indicated 50% to provide the optimal duty cycle. "IP" represents current segment adjustment. Seven segments are available for selection; a higher IP number indicates a larger I_{gap} value and faster processing speed but also reduces processing precision and increases nanoparticle size. The "EMERGENCY STOP" button is used for emergency shutdown and instantly halts the entire processing procedure, enabling accurate control of preparation time.

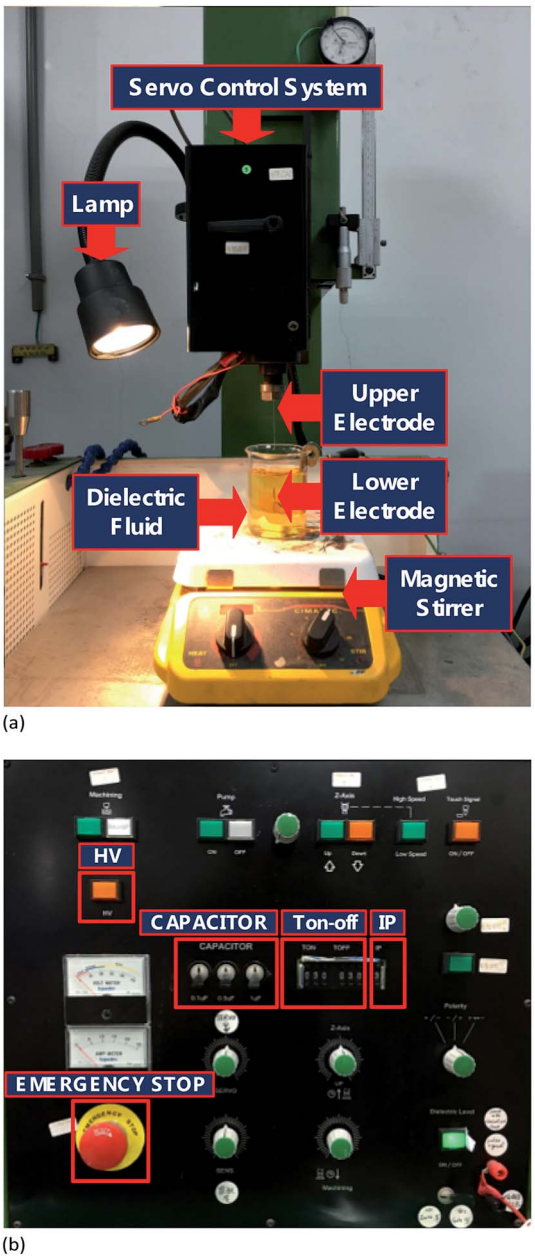

Fig. 1 Electric discharge machine: (a) preparation structure (b) control panel.

B Principle of ESDM in colloid preparation

Studies have indicated that ESDM can be applied in precision machining to improve processing precision. This method can also be implemented in nanocolloid preparation.[19,20] This involves generating spark discharge through the energy generated in a strong electric field when the distance between the two electrodes is adequately short, converting the electrical energy to thermal energy of 5000–6000 K[21] and using it to melt the workpiece and

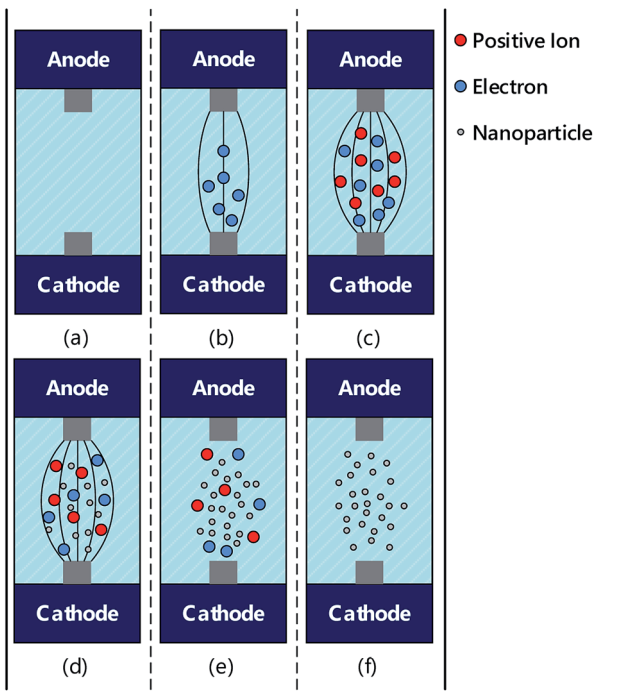

Fig. 2 Preparation of the nanocolloid through ESDM: (a) discharge preparation; (b) discharge initiation; (c) ionization; (d) melting; (e) discharge termination; (f) insulation restoration.

remove the material from its surface. Fig. 2 illustrates ESDM using the following steps: (a) attach the metallic workpieces firmly to the two electrodes and immerse them in the dielectric fluid while maintaining an extremely short distance between the metal components of two electrodes. At this point, the two electrodes remain insulated and without any gap voltage (V_{gap}) or current (I_{gap}). (b) The distance between the electrodes is slowly decreased, using the servo control system, until they are 30 μm apart, at which point the electric field is strong enough to remove the insulation properties of the dielectric fluid, causing numerous electrons to move from the cathode to the anode and triggering a chain reaction of discharge. (c) With the insulation properties of the fluid removed, the electrons flowing from the cathode to the anode impact the neutrons between the two electrodes, causing the neutrons to become cations through loss of their outer valence electrons. The electrons move rapidly to the anode, causing a second ionization and forming a low impedance channel, lowering V_{gap} and increasing I_{gap}. (d) Continuous ionization causes the positive and negative ions to continuously impact the two electrodes, forming an arc. In the process, the electric energy is instantly converted to produce a high level of thermal energy, which melts the surface of the metallic workpieces between the electrodes; the metallic nanoparticles that detach are then suspended in the dielectric fluid. (e) The procedure T_{off} occurs when the two electrodes cease generating voltage and the fluid recovers its insulation properties. The low impedance channel disappears, and the remaining nanoparticles cool in the fluid. At this point, $V_{gap} = 0$, and $I_{gap} = 0$. (f) T_{off} concludes a full cycle of electric discharge machining with the nanoparticles dispersed throughout the dielectric fluid. Subsequently, T_{on} marks the beginning of the next cycle. Thus, the discharge process is repeated for nanocolloid preparation.[22] Fig. 3 depicts the changes in V_{gap} and I_{gap}, and the six steps in Fig. 2 correspond to those in Fig. 3.

C ESDM nanocolloid preparation parameters

To investigate the effect of preparation conditions on platinum iodide nanocolloid concentration and suspension stability, five sets of T_{on}–T_{off} parameters were established as the preparation conditions for comparison. Table 1 lists the preparation parameters.

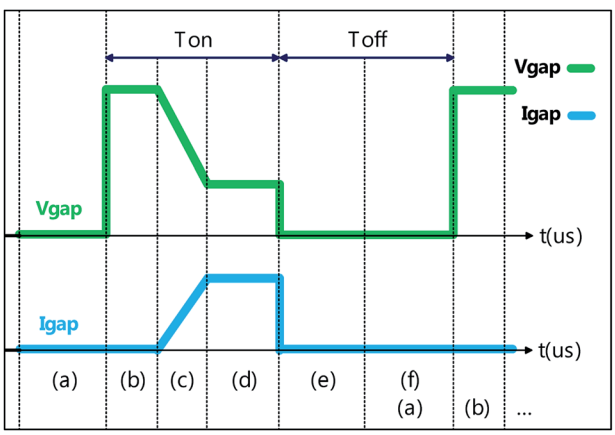

Fig. 3 V_{gap} and I_{gap} between the electrodes: (a) discharge preparation; (b) discharge initiation; (c) ionization; (d) melting; (e) discharge termination; (f) insulation restoration.

D Setting of apparatus

The completed nanocolloids were analyzed using a UV-vis (Thermo-Helios Omega, Thermo Fisher Scientific Inc, Waltham, MA, USA), a Zetasizer (Nano-ZS90, Malvern Zetasizer, Worcestershire, UK), and a TEM (JEM-2100F, JEOL Ltd, Japan). The UV-vis is used to measure the wavelengths and absorbance for comparing the nanocolloid concentrations. The start and stop wavelength are 190 and 600 nm under the scanning speed and interval of 240 nm min^{-1} and 1 nm. The Zetasizer was applied to measure the zeta potentials and nanoparticle sizes of the nanocolloids. If the absolute value of zeta potential is >30 mV, the suspension dispersion of the nanocolloid is deemed satisfactory due to the absence of agglomeration. The light source is He–Ne laser and the scattering angle is 90°. The dispersant is water with 25 °C in temperature, 1.330 in refractive index and 0.887 mPa s in viscosity. The TEM was employed to observe the microstructures of the nanocolloids. The energy is set to 200 kV and the amplification magnification is ×800 000.

3 Results and discussion

A Nanocolloid property analysis

Fig. 4(a) illustrates a prepared platinum iodide nanocolloid. The Tyndall effect is observed when a laser beam passes through the colloid, and a beam can be observed in the colloid in the direction perpendicular to the incident beam.[23] This is because the beam is scattered by suspended nanoparticles within the colloid. The platinum is insoluble in water and iodide is slightly soluble in water. So, platinum iodide is suspended in the water with the help of iodide. The lattice structure between platinum and platinum iodide is relatively close. With van der Waals force, platinum iodide can be attached to the surface of platinum. Platinum iodide itself is an ionic compound, iodide is slightly soluble in water and hydrogen bonds with water. The platinum iodide coated with nanoparticles with platinum as the core by hydrogen bonding can be suspended in water. The molecular structure is shown Fig. 4(b).

The UV-vis, Zetasizer, and TEM were used to examine the spectroscopy, zeta potentials, particle sizes, and microstructures of the nanocolloids. Fig. 5 depicts the UV-vis spectroscopy for nanocolloids prepared with the T_{on}–T_{off} parameters of 10–10, 30–30, 50–50, 70–70, and 90–90 μs. When the parameters were 10–10 μs, the maximal absorbance was 0.481 and 0.425, respectively, and the respective characteristic wavelengths were 285 and 350 nm. Accordingly, this set of parameters provided the optimal the ESDM process and the colloid concentration. Table 2 lists the UV-vis spectroscopic values of the colloids using the aforementioned five parameters, which similarly reveal a parameter of 10–10 μs to be optimal for nanocolloid preparation.

Table 3 lists the particle sizes and zeta potentials of the nanocolloids with the aforementioned T_{on}–T_{off} parameters. For

Table 1 Preparation parameters

Experimental parameter	Values
T_{on}–T_{off}	10–10, 30–30, 50–50, 70–70, 90–90 (μs)
Discharge time	5 min
Electrode diameter	Anode & cathode: pure platinum wire (99.5%): 1 mm
Dielectric fluid	DI water: 199.5 mL, liquid iodine (10% w/v): 0.5 mL
Volume of the dielectric fluid	Liquid iodine (250 ppm): 200 mL
Voltage	240 V
Temperature	25 °C (room temperature)
Atmospheric pressure	1 atm

parameters of 10–10 μs, the particle size of the nanocolloid was optimal (61.88 nm). A zeta potential absolute value higher than 30 mV indicates ideal colloid suspension stability.[24] Nanocolloid prepared using the parameters of 10–10, 30–30, and 50–50 μs exhibited satisfactory suspension stability. Accordingly, the parameter of 10–10 μs is optimal for nanocolloid preparation.

Fig. 6 depicts the Zetasizer analysis results of the nanocolloids prepared using the T_{on}–T_{off} parameters of 10–10 μs. As shown in Fig. 6(a), the zeta potential of the nanocolloid was −30.3 mV. Fig. 6(b) indicates nanoparticle size of 61.88 nm.

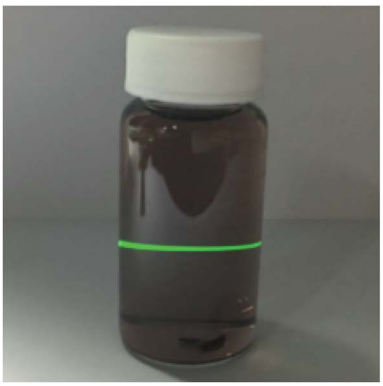

(a)

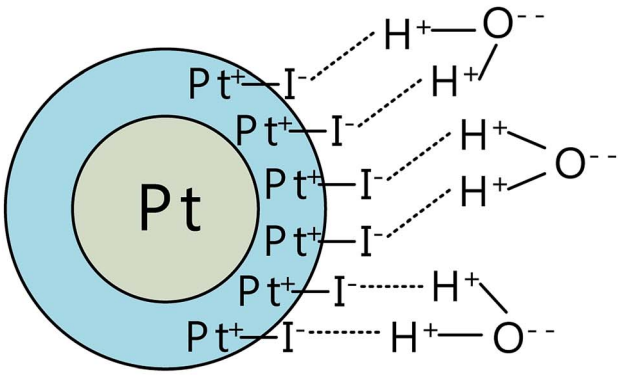

(b)

Fig. 4 Platinum iodide nanocolloid (a) Tyndall effect and (b) the molecular structure.

When the repulsive force between the particles is large, the absolute value of zeta potential will be greater than 30 mV. When the repulsive force between the particles is small, the particles are easy to agglomerate and combine and cause the particles become larger. The particle will precipitate at the bottom of the solution. The suspension stability is poor.[25] The particle prepared by ESDM is platinum iodide. It is physical chemistry method. The platinum is insoluble in water and iodide is slightly soluble in water. So, platinum iodide is suspended in the water with the help of iodide. Fig. 7 illustrates the TEM test results. The microstructure analysis of the nanocolloid through the TEM. Grey and black platinum iodide particles were detected, some with diameters of approximately 10 nm but most with diameters no larger than 5 nm. As shown in Fig. 7(a), for a scale bar of 10 nm, the nanoparticles were even more clearly visible. Fig. 7(b) depicts the analysis results using a scale

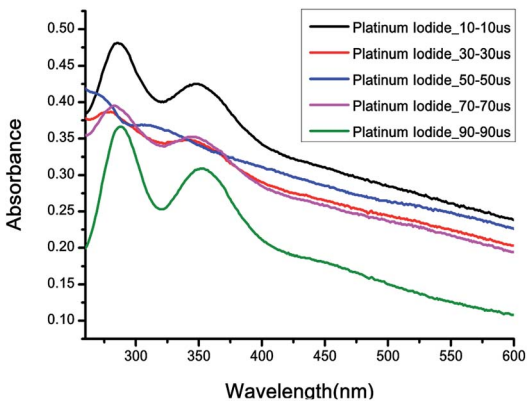

Fig. 5 UV-vis spectroscopy with various T_{on}–T_{off} parameters.

Table 2 UV absorbance with various T_{on}–T_{off} parameters

T_{on}–T_{off} (μs)	Absorbance
10–10	0.481, 0.425
30–30	0.387, 0.348
50–50	0.419, 0.369
70–70	0.395, 0.352
90–90	0.366, 0.309

Table 3 Particle sizes and zeta potentials with various T_{on}–T_{off} parameters

T_{on}–T_{off} (μs)	Size distribution (r.nm)	Zeta potential (mV)
10–10	30.94	−30.3
30–30	32.37	−32.6
50–50	41.88	−32.3
70–70	32.41	−29.7
90–90	30.98	−28.2

bar of 5 nm, in which lattice lines with 0.226 nm widths were observed in the nanoparticles.

B Discussion

In summary, with T_{on}–T_{off} parameters of 10–10 μs, the UV absorbance of the nanocolloid was maximized at 0.481 and 0.425, respectively. The characteristic wavelengths were 285 and 350 nm, respectively. The zeta potential of the nanocolloid was −30.3 mV. As examined through the TEM, the sizes of all nanoparticles were no larger than 10 nm. Accordingly, with the

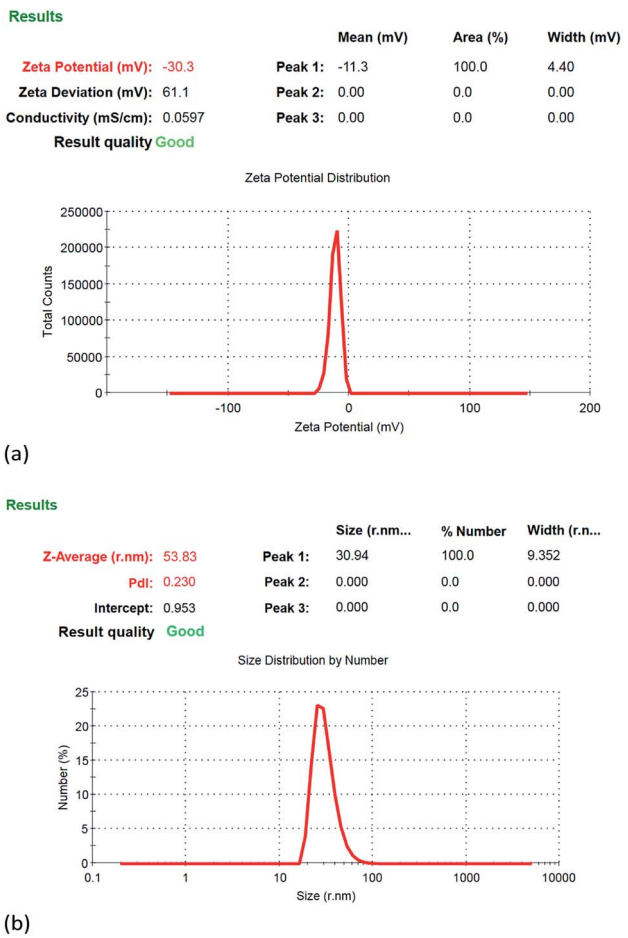

Fig. 6 ESDM-prepared platinum iodide nanocolloid property analysis: (a) zeta potential (b) size distribution.

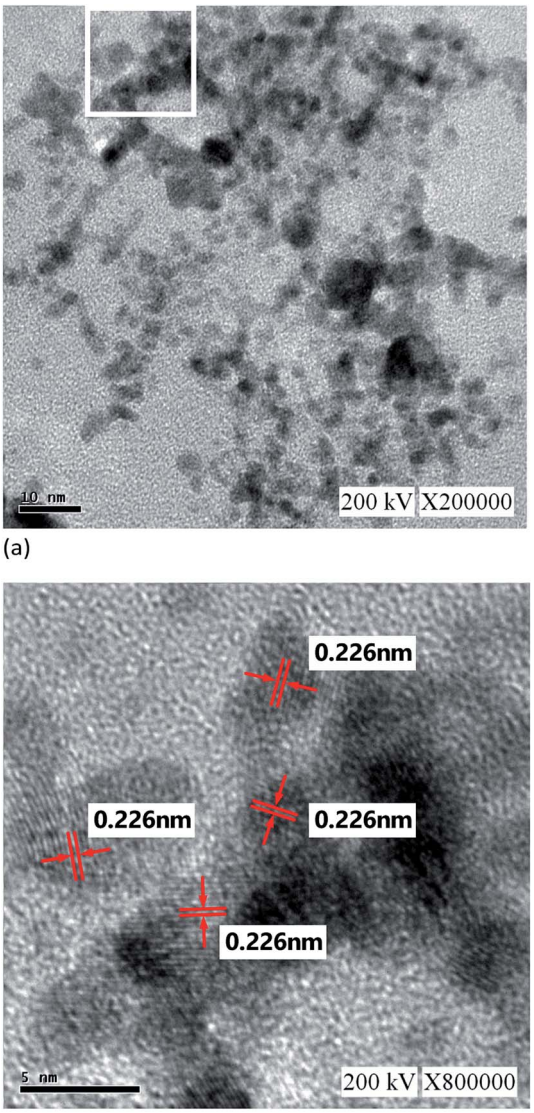

Fig. 7 TEM observation: (a) scale 10 nm (b) scale 5 nm.

T_{on}–T_{off} parameters of 10–10 μs, the nanocolloid concentration was maximized, its nanoparticle size was minimized, and its suspension stability was optimized. Thus, the parameters of 10–10 μs provide the optimal condition for preparing platinum iodide nanocolloids.

4 Conclusions

This study employed ESDM to prepare platinum iodide nanocolloids. Five sets of T_{on}–T_{off} parameters were applied, namely, 10–10, 30–30, 50–50, 70–70, and 90–90 μs, to identify the optimal parameter settings for nanocolloid preparation. A UV-vis spectroscope, a Zetasizer, and a TEM were employed to examine the nanocolloids' properties. The conclusion is as follows:

(1) a nanocolloid with satisfactory suspension stability was successfully created using 250 ppm liquid iodine dielectric fluid in an EDM.

(2) According to the TEM examination results, the nanocolloid's nanoparticle size was no larger than 10 nm.

(3) The T_{on}–T_{off} parameters of 10–10 μs provide the optimal preparation conditions. With this parameter set, the nanocolloid featured characteristic wavelengths of 285 and 350 nm, respectively. Absorbance was 0.481 and 0.425 nm, respectively. The zeta potential of the nanocolloid was −30.3 mV.

(4) ESDM is a physical and green nanocolloid preparation method, which is time-efficient and environmentally friendly. Platinum iodide nanocolloids prepared by ESDM are more suitable for applying in medicine, various cancer and drug treatments to avoid damage to the human body and pollute environments.

Conflicts of interest

There are no conflicts to declare.

Acknowledgements

The authors would like to thank the Precision Research and Analysis Center, National Taipei University of Technology for technically supporting this research. The authors would also like to thank the Ministry of Science and Technology (MOST 108-2221-E-027-050-) for financial support of this research.

References

1 J. C. Chou, W. Y. Hsu, Y. H. Liao, C. H. Lai, Y. J. Lin, P. H. You and Y. H. Nien, Photovoltaic analysis of platinum counter electrode modified by graphene oxide and magnetic beads for dye-sensitized solar cell, *IEEE Trans. Semicond. Manuf.*, 2017, **30**(3), 270–275.

2 Y. J. Lee and J. Y. Park, Highly selective and sensitive electrochemical detection of dopamine using a Nafion coated hybrid macroporous gold modified electrode with platinum nanoparticles, *IEEE Transactions on NanoBioscience*, 2011, **10**(4), 250–258.

3 P. W. Jacobs, S. J. Wind, F. H. Ribeiro and G. A. Somorjai, Nanometer size platinum particle arrays: catalytic and surface chemical properties, *Surf. Sci.*, 1997, **372**(1–3), L249–L253.

4 J. Qu, F. Ye, D. Chen, Y. Feng, Q. Yao, H. Liu and J. Yang, Platinum-based heterogeneous nanomaterials via wet-chemistry approaches toward electrocatalytic applications, *Adv. Colloid Interface Sci.*, 2016, **230**, 29–53.

5 A. Zribi, M. Barthes, S. Bégot, F. Lanzetta, J. Y. Rauch and V. Moutarlier, Design, fabrication and characterization of thin film resistances for heat flux sensing application, *Sens. Actuators, A*, 2016, **245**, 26–39.

6 K. Li, G. S. M. Tong, Q. Wan, G. Cheng, W. Y. Tong, W. H. Ang and C. M. Che, Highly phosphorescent platinum(II) emitters: photophysics, materials and biological applications, *Chem. Sci.*, 2016, **7**(3), 1653–1673.

7 R. Czarnomysy, A. Surażyński, A. Muszynska, A. Gornowicz, A. Bielawska and K. Bielawski, A novel series of pyrazole-platinum(II) complexes as potential anti-cancer agents that induce cell cycle arrest and apoptosis in breast cancer cells, *J. Enzyme Inhib. Med. Chem.*, 2018, **33**(1), 1006–1023.

8 D. Wang and S. J. Lippard, Cellular processing of platinum anticancer drugs, *Nat. Rev. Drug Discovery*, 2005, **4**(4), 307.

9 L. Kelland, The resurgence of platinum-based cancer chemotherapy, *Nat. Rev. Cancer*, 2007, **7**(8), 573.

10 J. B. Vermorken, R. Mesia, F. Rivera, E. Remenar, A. Kawecki, S. Rottey and F. Peyrade, Platinum-based chemotherapy plus cetuximab in head and neck cancer, *N. Engl. J. Med.*, 2008, **359**(11), 1116–1127.

11 A. G. Quiroga, M. Cama, N. Pajuelo-Lozano, A. Álvarez-Valdés and I. S. Perez, New Findings in the Signaling Pathways of cis and trans Platinum Iodido Complexes' Interaction with DNA of Cancer Cells, *ACS Omega*, 2019, 21855–21861.

12 Y. Kojima, K. I. Suzuki and Y. Kawai, Hydrogen generation from lithium borohydride solution over nano-sized platinum dispersed on $LiCoO_2$, *J. Power Sources*, 2006, **155**(2), 325–328.

13 A. Dolatshahi-Pirouz, K. Rechendorff, M. B. Hovgaard, M. Foss, J. Chevallier and F. Besenbacher, Bovine serum albumin adsorption on nano-rough platinum surfaces studied by QCM-D, *Colloids Surf., B*, 2008, **66**(1), 53–59.

14 K. H. Tseng, Y. H. Lin, D. C. Tien, H. C. Ku and L. Stobinski, Stability analysis of platinum nanoparticles prepared by ESDM in deionised water, *Micro Nano Lett.*, 2018, **13**(11), 1545–1549.

15 P. L. Bigliardi, S. A. L. Alsagoff, H. Y. El-Kafrawi, J. K. Pyon, C. T. C. Wa and M. A. Villa, Povidone iodine in wound healing: a review of current concepts and practices, *Int. J. Surg.*, 2017, **44**, 260–268.

16 H. Tian, T. Gao, X. Li, X. Wang, C. Luo, X. Fan and C. Wang, High power rechargeable magnesium/iodine battery chemistry, *Nat. Commun.*, 2017, **8**(1), 1–8.

17 K. H. Tseng, Y. S. Lin, C. Y. Chang and M. Y. Chung, A Study of a PID Controller Used in a Micro-Electrical Discharge Machining System to Prepare TiO_2 Nanocolloids, *Nanomaterials*, 2020, **10**(6), 1044.

18 W. S. Yang, B. W. Park, E. H. Jung, N. J. Jeon, Y. C. Kim, D. U. Lee and S. I. Seok, Iodide management in formamidinium-lead-halide–based perovskite layers for efficient solar cells, *Science*, 2017, **356**(6345), 1376–1379.

19 K. H. Tseng, H. C. Ku, D. C. Tien and L. Stobinski, Novel Preparation of Reduced Graphene Oxide–Silver Complex using an Electrical Spark Discharge Method, *Nanomaterials*, 2019, **9**(7), 979.

20 K. H. Tseng, M. Y. Chung and J. L. Chiu, Suspension stability of nano-Au and nano-Ag colloids prepared by electrical spark discharge method, *J. Cluster Sci.*, 2017, **28**(5), 2653–2668.

21 M. Gostimirovic, P. Kovac, M. Sekulic and B. Skoric, Influence of discharge energy on machining characteristics in EDM, *J. Mech. Sci. Technol.*, 2012, **26**(1), 173–179.

22 R. K. Sahu, S. S. Hiremath, P. V. Manivannan and M. Singaperumal, Generation and characterization of copper nanoparticles using micro-electrical discharge machining, *Mater. Manuf. Processes*, 2014, **29**(4), 477–486.

23 J. W. Liaw, S. W. Tsai, H. H. Lin, T. C. Yen and B. R. Chen, Wavelength-dependent Faraday–Tyndall effect on laser-induced microbubble in gold colloid, *J. Quant. Spectrosc. Radiat. Transfer*, 2012, **113**(17), 2234–2242.

24 K. H. Tseng, H. C. Ku, D. C. Tien and L. Stobinski, Parameter control and concentration analysis of graphene colloids prepared by electric spark discharge method, *Nanotechnol. Rev.*, 2019, **8**(1), 201–209.

25 W. Huo, X. Zhang, K. Gan, Y. Chen, J. Xu and J. Yang, Effect of zeta potential on properties of foamed colloidal suspension, *J. Eur. Ceram. Soc.*, 2019, **39**(2–3), 574–583.